Molecular Cell *23*, 509–521, August 18, 2006 ©2006 Elsevier Inc. DOI 10.1016/j.molcel.2006.06.021

Identification of Early Intermediates of Caspase Activation Using Selective Inhibitors and Activity-Based Probes

Alicia B. Berger,[1,3] Martin D. Witte,[4] Jean-Bernard Denault,[5] Amir Masoud Sadaghiani,[1] Kelly M.B. Sexton,[1] Guy S. Salvesen,[5] and Matthew Bogyo[1,2,*]

[1] Department of Pathology
[2] Department of Microbiology and Immunology
[3] Cancer Biology Graduate Program
Stanford University School of Medicine
300 Pasteur Drive
Stanford, California 94305
[4] Bio-organic Synthesis
Leiden Institute of Chemistry
Leiden University
2300 RA Leiden
The Netherlands
[5] Burnham Institute for Medical Research
10901 North Torrey Pines Road
La Jolla, California 92037

Summary

Caspases are cysteine proteases that are key effectors in apoptotic cell death. Currently, there is a lack of tools that can be used to monitor the regulation of specific caspases in the context of distinct apoptotic programs. We describe the development of highly selective inhibitors and active site probes and their applications to directly monitor executioner (caspase-3 and -7) and initiator (caspase-8 and -9) caspase activity. Specifically, these reagents were used to dissect the kinetics of caspase activation upon stimulation of apoptosis in cell-free extracts and intact cells. These studies identified a full-length caspase-7 intermediate that becomes catalytically activated early in the pathway and whose further processing is mediated by mature executioner caspases rather than initiator caspases. This form also shows distinct inhibitor sensitivity compared to processed caspase-7. Our data suggest that caspase-7 activation proceeds through a previously uncharacterized intermediate that is formed without cleavage of the intact zymogen.

Introduction

The clan CD cysteine proteases known as caspases play a pivotal role in apoptosis, a tightly regulated form of programmed cell death essential for tissue homeostasis and elimination of damaged cells. Improper regulation of apoptosis is estimated to play a role in 70% of human diseases, including cancer, certain neurodegenerative diseases, and reperfusion injury after ischemia (Reed, 1998). Thus, tools to study caspases in both a basic and clinical setting are in high demand.

Caspases are present in the cytosol as inactive zymogens that become activated in response to specific death stimuli. Once activated, initiator caspases (caspase-8, -9, and -10) cleave and activate executioner caspases (caspases-3 and -7). There are two primary pathways used to establish the cell death program. In general, the intrinsic pathway mediates response to cellular stress, such as DNA damage, and results in the activation of initiator caspase-9, whereas the extrinsic pathway is triggered by extracellular signals such as Fas binding to its cognate receptor and leads to activation of initiator caspase-8. In both pathways, initiator caspases cleave and activate downstream executioner caspases (Boatright et al., 2003; Denault and Salvesen, 2002; Garcia-Calvo et al., 1998).

Because intrinsic and extrinsic apoptosis signals culminate in the activation of the same executioner caspases, it has remained difficult to define the contribution of each pathway to apoptotic processes in vivo. Furthermore, activities of the executioner caspases increase over time, causing them to dominate most nonspecific caspase activity assays. This has prevented the detailed analysis of the kinetics of early activation events. In addition, surprisingly few tools are available for directly monitoring individual caspase activities in complex proteomes. Current strategies depend largely on antibody-based methods that can detect cleavage events of specific caspases. However, proteolytic cleavage is often not required for activation, and a number of endogenous inhibitors exist that serve to control caspase activity through complex posttranslational mechanisms (Deveraux et al., 1999). Alternatively, caspase-targeted substrates and inhibitors can be used to directly monitor caspase activity. However, the value of virtually all commercial reagents is limited by their overall poor selectivity (James et al., 2004).

Here, we describe the development and application of highly selective inhibitors and activity-based probes (ABPs) for caspases-3, -7, -8, and -9. We used a positional scanning combinatorial library (PSCL) approach to screen pools of peptide acyloxymethyl ketones (AOMKs) containing both natural and nonnatural amino acids for activity against a number of purified recombinant caspases. These screens identified structural elements at multiple positions on the peptide scaffold that could be modulated to control inhibitor specificity toward target caspases. Based on this screening data, we designed individual optimized covalent inhibitors that could also be equipped with various tags for use as ABPs (Figure 1). Using this strategy, we have developed several caspase-selective inhibitors and probes capable of specific inhibition and labeling of both recombinant and endogenous caspases. These reagents were applied to studies of the kinetics of caspase activation in both a cell-free system in which intrinsic apoptosis could be activated by addition of cytochrome c and dATP and in intact cells where apoptosis could be activated by multiple different stimuli. Using both general ABPs and specific inhibitors, we have identified a full-length, uncleaved form of caspase-7 that becomes catalytically activated upon induction of apoptosis. This intermediate species is converted to mature processed forms by both caspase-3 and fully mature forms of caspase-7 itself. Interestingly, we find that active

*Correspondence: mbogyo@stanford.edu

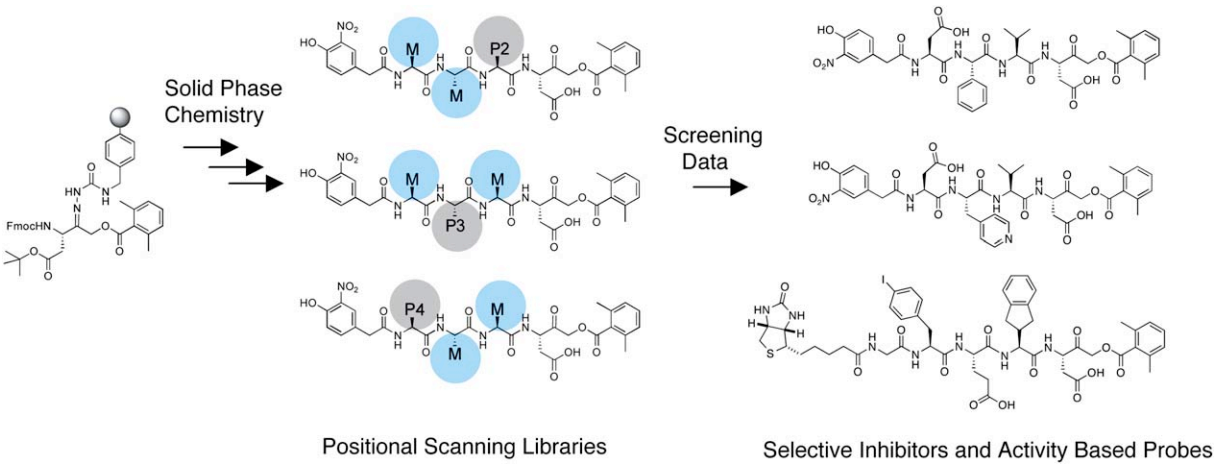

Figure 1. Development of Caspase-Specific Inhibitors and Active Site Probes

Solid phase chemistry was used to synthesize positional scanning combinatorial libraries (PSCLs) of nitrophenyl acetate (NP) capped peptide acyloxymethyl ketones (AOMKs). For all libraries, the P1 position directly adjacent to the reactive AOMK group was held constant as aspartic acid due to the strict cleavage requirements of caspases at this residue. One of the three remaining positions was also held constant (gray circles) as a single natural (a total of 19 excluding cysteine and methionine plus norleucine) or nonnatural amino acid (from a set of 41 nonnaturals—see the Supplemental Data), whereas the other positions contained isokinetic mixtures of the natural amino acids (blue circles). Single inhibitor compounds were selected after screening to determine the binding preference of individual caspases. Tags, such as biotin, were added in place of the nitrophenyl acetate cap of selective inhibitors to make activity-based probes (ABPs).

full-length caspase-7 shows differential inhibitor sensitivity compared to all other processed forms of the enzyme, suggesting that it is a distinct intermediate in the caspase-7 activation pathway.

Results

Inhibitor Library Design

Past studies of substrate specificity of multiple caspase family members have focused on the use of PSCLs of fluorogenic peptide substrates (Backes et al., 2000; Thornberry et al., 1997). Such PSCL methods can be used to rapidly and efficiently determine the contribution of a single amino acid in a substrate or inhibitor scaffold to active site binding (Greenbaum et al., 2000, 2002; Nazif and Bogyo, 2001). Initial libraries of 3-nitro-4-hydroxy phenyl acetyl (NP) capped tetrapeptide AOMKs were synthesized by using solid phase methods originally developed by Ellman and coworkers (Lee et al., 1999) and optimized for extended peptide AOMKs by our group (Kato et al., 2005) (Figure 1). For all libraries, the P1 position directly adjacent to the reactive AOMK group was held constant as aspartic acid in order to satisfy the strict P1 specificity requirements of caspases (Stennicke et al., 2000). In all libraries, one of the three remaining positions was held constant as a single natural (a total of 19 excluding cysteine and methionine plus norleucine) or nonnatural amino acid (from a set of 41 nonnaturals—see the Supplemental Data available with this article online) whilee the other positions contained mixtures of the natural amino acids. Thus, screening of all 60 amino acids was accomplished by the synthesis of three PSCLs composed of 180 sublibraries that contained 361 compounds each. All inhibitors and probes contain the dimethylbenzoic acid AOMK warhead that has been described as optimal for caspase-targeted ABPs (Kato et al., 2005; Thornberry et al., 1994).

Inhibitor Library Screening and Design of Selective Inhibitors

The complete set of libraries were screened in triplicate by a simple fluorogenic peptide substrate assay in which residual enzyme activity was calculated from the ratio of normalized fluorescence signal of inhibited and control, noninhibited samples. To aid in data analysis, residual enzyme activity values were organized by using a hierarchical clustering algorithm that converts residual activity values into a color format, or heat map, where red and blue colors represent 0% and 100% residual activity, respectively. Generated heat maps (Figure S1) represent "affinity fingerprints" (Greenbaum et al., 2002) of the preferred amino acids in the inhibitor specificity region for each of the caspases and were used to design selective inhibitors. Inhibitor specificity for the natural amino acid sublibraries agreed very closely with previous reported substrate specificity data for the caspases, suggesting that the inhibitors bind in a manner similar to substrates (Thornberry et al., 1997).

One of the primary limitations of the PSCL approach is the inability of the libraries to predict the importance of collaborative binding interactions for multiple specificity sites on a given inhibitor. Thus, we decided to substitute residues identified from our screening data into an optimal substrate sequence to enhance selectivity and potency toward a given caspase target. We initially chose AOMK versions of the optimal substrate sequences used in a number of commercially available "selective" inhibitors as our starting scaffolds. However, the inhibitors AB07 (NP-LEHD-AOMK, caspase-9), AB08 (NP-LETD-AOMK, caspase-8), and AB09 (NP-DEVD-AOMK, caspase-3) lacked selectivity (Table 1). In particular, NP-LEHD-AOMK, which was designed to target caspase-9, showed more rapid inhibition of caspase-8. Similarly, NP-DEVD-AOMK, which was designed to target caspase-3, showed strong activity toward caspase-8.

Table 1. $K_{i(app)}$ Values for Select AB Compounds

Target Caspase	Compound	Specificity Region	$K_{i(app)}$ [$M^{-1}s^{-1}$]			
			Caspase-3	Caspase-7	Caspase-8	Caspase-9
3, 7, 8, 9	ZVAD-fmk	V-A-D	25,922	<5000	20,3286	<5000
	KMB01	E-V-D	577,913	288,213	164,052	175,210
	AB11	D-E-P-D	2,482,333	199,341	580,547	47,362
	AB28	6-E-8-D	1,020,213	272,619	817,077	300,767
3,7	AB09	D-E-V-D	10,922,261	1,529,040	1,077,839	<5000
	AB06	D-3-V-D	7,456,511	968,070	32,909	NI
	AB12	D-29-V-D	5,652,900	783,840	271,626	NI
	AB13	D-34-V-D	3,416,050	279,519	<5000	NI
	AB16	26-3-V-D	484,495	24,185	121,650	NI
	AB17	26-E-V-D	781,733	448,155	126,323	NI
8	AB08	L-E-T-D	127,835	19,424	599,788	<5000
	AB20	29-E-T-D	570,900	181,332	1,071,401	41,300
	AB18	31-E-T-D	216,040	234,945	572,012	12,320
	AB19	31-E-23-D	179,086	42,994	396,225	NI
9	AB07	L-E-H-D	75,295	10,447	506,912	20,141
	AB38	P-L-A-D	46,108	27,814	19,676	18,004
	AB40	I-L-A-D	261,470	11,256	35,174	48,867
	AB41	I-L-38-D	1,582,350	69,317	49,815	35,779
	AB42	I-F-P-D	892,045	42,594	22,544	44,709

$K_{i(app)}$ values for select AB compounds. $K_{i(app)}$ values (also called K_{ass} or $K_{obs/I}$) represent the speed of inhibitor binding to a target enzyme. Units are [$M^{-1}s^{-1}$]. NI indicates no inhibition at concentrations tested. Parent compounds AB09, AB08, and AB07 contain the optimal substrate specificity sequences for caspases 3/7, 8, and 9, respectively, as determined by Thornberry and colleagues (Thornberry et al., 1997).

Therefore, we began by replacing one, two, or all three of the P2–P4 positions in these parent substrates with optimal residues from our screening data. In addition, we made use of residues that selected against binding to a subset of caspase targets, thereby increasing selectivity (Table 1 and Table S1).

For caspase-3, we chose to focus on changes in the P3 position of the optimal DEVD sequence, as there were a number of both natural and nonnatural residues that were well tolerated by caspase-3 and -7 and not caspases-8 and -9. Interestingly, placement of NN3 and NN34 in the P3 position was sufficient to generate highly potent and selective caspase-3 and -7 inhibitors. Thus, we selected AB06 and AB13 as our optimal caspase-3 inhibitors. Both of these compounds were converted to biotin-labeled probes (bAB06 and bAB13) by replacement of the NP cap with a long-chain biotin moiety. Importantly, these probes retained their selectivity for caspase-3 and -7 (Table S1).

To design compounds that target extrinsic initiator caspase-8, we initially chose to focus on the P2 and P4 positions due to its narrow selectivity preference in the P3 position. Substitution of the P4 Leu for the caspase-8 optimal NN29 resulted in a compound (AB20) with the highest kinetic inhibition constants for caspase-8 that we have measured so far. However, this increase in potency came at the price of reduced selectivity relative to both caspase-9 and -3. Further substitution of the P2 position of AB20 with the nonnatural amino acid 23 resulted in a compound (AB19) that retained relatively good potency for caspase-8 and showed no measurable activity for caspase-9. Although this compound still retained a reasonable level of activity against caspase-3, this was not a major concern, as this crossreactivity could be blocked by pretreatment of a sample with a selective caspase-3 inhibitor allowing specific labeling of caspase-8. AB19 therefore served as our optimal lead and was converted to the biotin-labeled probe (bAB19) that retained its caspase-8 selectivity (Table 1 and Table S1).

Development of caspase-9 selective inhibitors was much more challenging. Because the initial substrate-optimized sequence LEHD showed greater potency for caspase-8 than -9, we decided to begin by completely redesigning the peptide sequence using optimal residues in the P2–P4 positions. Of the seven compounds selected as optimal caspase-9 inhibitors, only a few showed activity against caspase-9 and many actually showed preference for caspase-8. This is most likely the result of vast differences in the overall catalytic efficiencies of the two enzymes. Thus, the caspase-9-targeted inhibitors that exhibited some selectivity in kinetic assays show no selectivity in competition assays because high concentrations are required for complete inhibition. We therefore believe that screening of recombinant enzymes may not be optimal, and a more thorough analysis using endogenous caspase-9 that has been activated in a cytosolic extract may be required to develop fully optimized caspase-9 selective inhibitors and probes. Nonetheless, we were able to improve upon the current LEHD sequence and generate compounds with some degree of selectivity for caspase-9 (AB38 and AB42).

Finally, we selected several general caspase compounds based on optimal sequences for all caspases tested. The predicted optimal 6E8D sequence as the free amino product (NH_2-6E8D; AB28) showed broad inhibition of all caspases. Similarly, the DEPD sequence (AB11) showed comparable inhibition kinetics to the previously reported general probe KMB01.

Selectivity of Caspase Inhibitors and ABPs for Recombinant and Endogenous Caspases

To further demonstrate overall selectivity and potency of our optimized compounds, we used an indirect competition assay in which recombinant caspase-3, -7, -8,

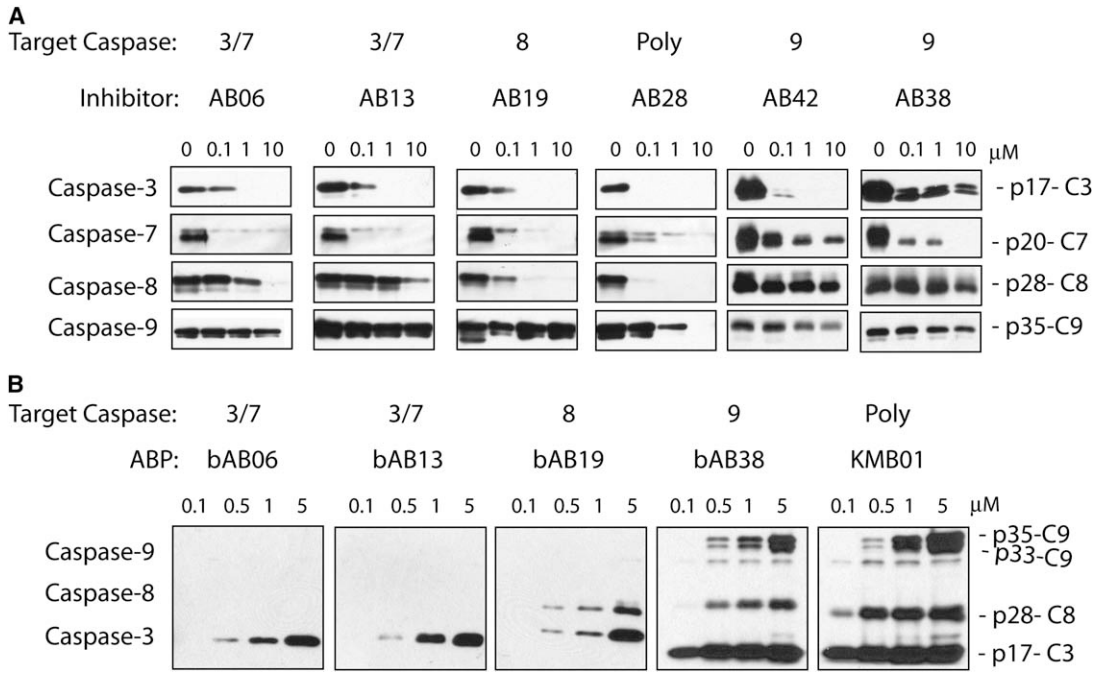

Figure 2. Analysis of Inhibitor and Probe Selectivity by Indirect Competition and Direct Labeling of Recombinant Caspases

(A) Indirect competition of a panel of inhibitors with the general caspase probe KMB01. Individual caspases-3, -7, -8, and -9 (100 nM each) were incubated with the indicated inhibitors for 30 min followed by a 30 min incubation with KMB01. Samples were analyzed by SDS-PAGE, and residual active site labeling was visualized by biotin blotting using streptavidin-HRP.

(B) Direct labeling of caspase active sites using specific ABPs. Equal amounts of active caspases-3, -8, and -9 (100 nM) were incubated together with increasing concentrations of each of the indicated biotinylated active site probes for 30 min. Active site labeling was visualized by SDS-PAGE analysis followed by biotin blotting using streptavidin HRP.

and -9 were individually preincubated with inhibitors at a range of concentrations and residual activity was measured by addition of the general caspase probe KMB01. Overall, the competition data mirrored the kinetic data with only minor differences for some compounds (i.e., AB06 and AB13 show slightly different selectivity for caspase-3 and -7) that reflect the inherent difference in the two assays. Whereas the kinetic assay allows measurement of kinetic binding constants, the competition method is a simple end point assay that only provides a single static inhibition value. Regardless of these differences, caspase-3 and -8-targeted compounds showed specific inhibition of the desired targets (Figure 2). As expected, the caspase-9-targeted compounds AB38 and AB42 showed only a minimal degree of selectivity for caspase-9 over caspase-8. The general inhibitor AB28 blocked labeling of all four caspase targets with caspase-9, requiring the highest concentration to obtain complete inhibition.

To test the overall selectivity of our sequences and to determine their utility as selective ABPs, we monitored direct labeling of a mixture of recombinant caspases by biotinylated versions of AB06, AB13, AB19, and AB38. Probes were added at a range of concentrations to normalized mixtures of recombinant caspase-3, -8, and -9. Both bAB06 and bAB13 selectively labeled caspase-3, whereas bAB19 labeled caspase-8 with no crossreaction with caspase-9 even at concentrations as high as 10 μM (Figure 2B). Not surprisingly, bAB38 labeled both caspase-8 and caspase-9.

We next tested the selectivity of our probes against endogenous caspase targets in a complex proteome. The intrinsic apoptosis pathway can be activated in cytosolic extract by addition of cytochrome c and dATP. This system allows temporal control of the apoptotic pathway and leads to activation of caspase-9 as well as caspase-3 and -7 (Liu et al., 1996). Upon activation of cell-free apoptosis for 10 min, the general probe KMB01 labeled a 35 kDa caspase-9 species and the two primary mature forms of caspase-3 at 17 and 20 kDa as well the 33 kDa full-length N peptide processed and 20 kDa mature forms of caspase-7 (Figure 3A). The identities of these labeled species were confirmed by immunoprecipitation experiments using specific antisera (Figures 3B and 4B). The two caspase-3-selective probes bAB06 and bAB13 efficiently and selectively labeled the mature caspase-3 and -7 species at probe concentrations ranging from 10 nM to 10 μM (Figures 3A and 3B).

Because cytosolic extracts induced to undergo intrinsic apoptosis through addition of cytochrome c/dATP do not contain detectable amounts of active endogenous caspase-8, we evaluated selectivity of the caspase-8 and -9-targeted probes by adding exogenous, active recombinant caspase-8 to the extracts at a concentration (50 nM) similar to reported endogenous levels of active caspase-8 (Boatright et al., 2003). The general probe KMB01 showed strong labeling of endogenous caspases-3, -7, and -9 as well as exogenously added caspase-8 in cytochrome c/dATP-stimulated

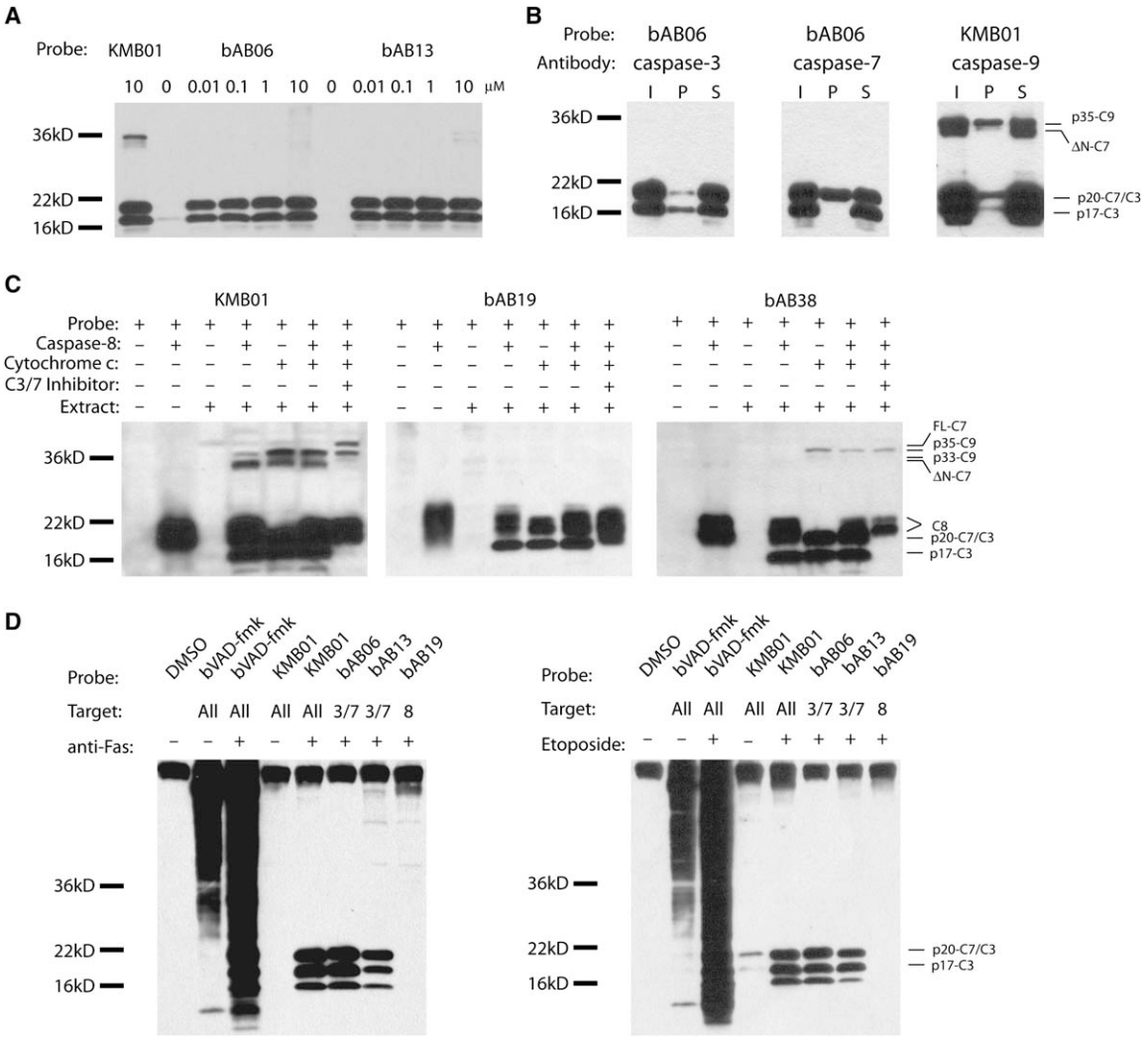

Figure 3. Selective Labeling of Endogenous Caspases in Cell Extracts and Live Cells with Active Site Probes

(A) Hypotonic 293 cytosolic extracts were induced to undergo intrinsic apoptosis by addition of cytochrome c/dATP, KMB01, bAB06, or bAB13 was added 10 min after activation, and labeling of caspase active sites was carried out for 30 min. Samples were analyzed by SDS-PAGE followed by biotin blotting using streptavidin-HRP.

(B) The identity of individual caspases was confirmed via immunoprecipitation using specific antisera for caspases-3, -7, and -9 (also see Figure 4B for immunoprecipitation of caspases-3 and -7 after KMB01 labeling). Extracts (293) were activated with cytochrome c/dATP for 10 min, labeled by addition of indicated probes (100 nM final concentration for bAB06 and bAB13 and 10 μM final concentration for KMB01), and labeled caspases were precipitated by using specific antisera as described in the Experimental Procedures section. I is input, P is pellet, S is supernatant after specific precipitation.

(C) Recombinant caspase-8 (50 nM) was either directly labeled or added to cell extracts (293) with or without cytochrome c/dATP activation and then labeled with the indicated probes (10 μM final concentration). The caspase-3-selective inhibitor AB06 (10 μM final concentration) was also added 10 min prior to probe addition to indicated samples. Labeling of caspases was monitored by SDS-PAGE followed by bitoin blotting with streptavidin-HRP.

(D) Labeling of endogenous caspase-3 and -7 in intact Jurkat cells induced to undergo apoptosis through etoposide or anti-Fas treatment. Cells (3×10^6) were incubated with apoptosis inducers for 15 hr and then labeled by incubation for an additional 2 hr with the panel of probes indicated. b-VAD-fmk, KMB01, and bAB19 were used at a 10 μM final concentration. bAB06 and bAB13 were used at 1 μM final concentration.

extracts (Figure 3C). Similar labeling experiments using high concentrations of the caspase-8-selective probe bAB19 confirmed that it efficiently labeled the exogenous active caspase-8 and, to a lesser extent, caspase-3 while showing no labeling of caspase-9 even after stimulation with cytochrome c/dATP. The caspase-9-targeted probe bAB38 showed labeling of caspase-9 with crossreactivity toward caspases-3 and -8.

As a final test of the utility of the probes, we examined their ability to label endogenous caspase targets in intact cells induced to undergo apopotosis by either extrinsic (anti-Fas antibody) or intrinsic (etoposide) signals. The biotinylated probes KMB01, bAB06, and bAB13 produced robust labeling of downstream caspases-3 and -7 in anti-Fas and etoposide-treated Jurkat cells (Figure 3D). Furthermore, this labeling was achieved at relatively low concentrations of probe (1 μM), suggesting

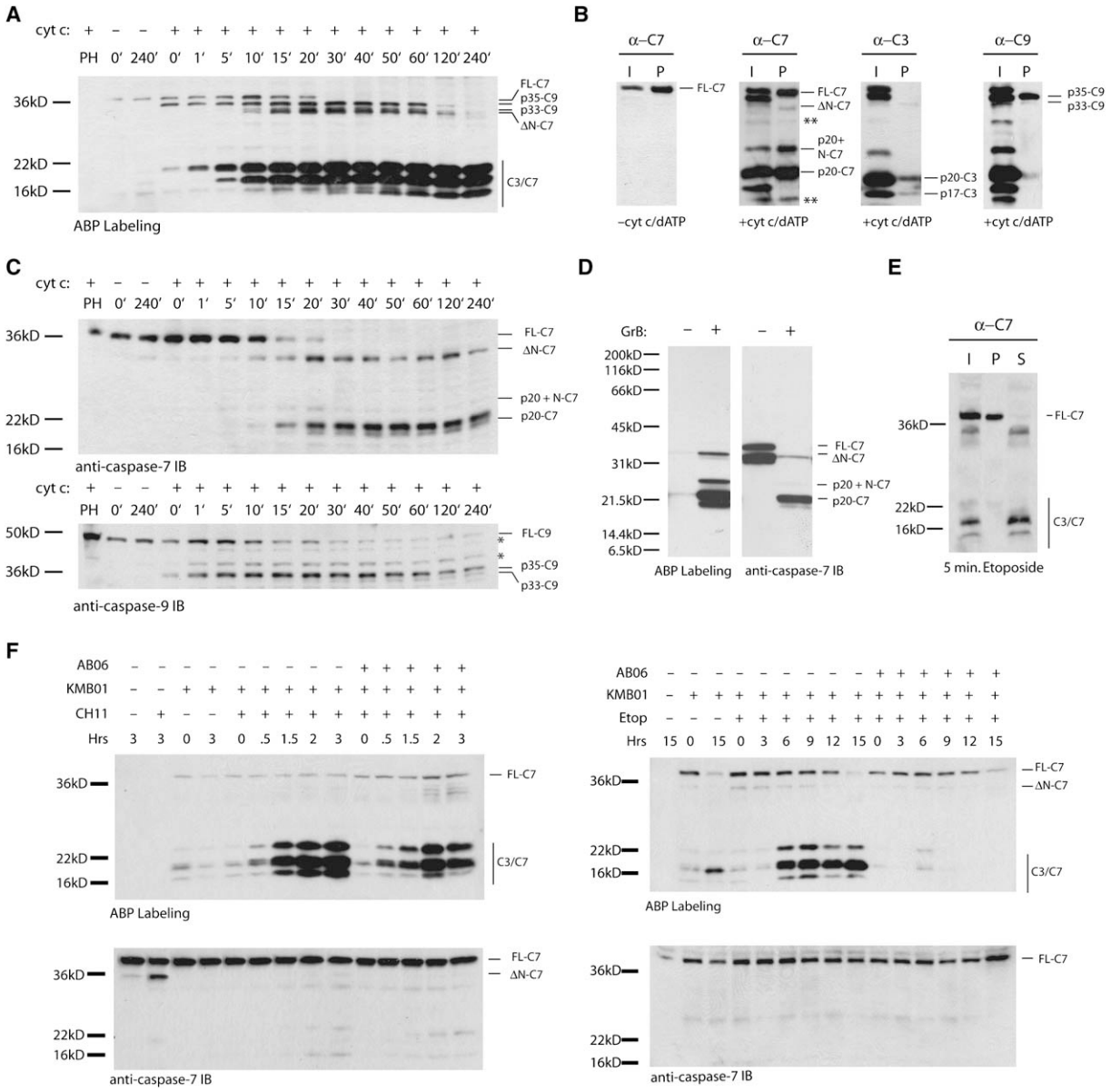

Figure 4. Identification of a Caspase-7 Activation Intermediate in Apoptotic Cell Extracts and Intact Cells

(A) Cytosolic extracts (293) were induced to undergo intrinsic apoptosis by addition of cytochrome c/dATP for the indicated times. At the end of each time point, the general caspase probe KMB01 was added and extracts were incubated for an additional 30 min at 37°C. Labeled caspase active sites were visualized by SDS-PAGE analysis followed by blotting for biotin with streptavidin-HRP.

(B) Immunoprecipitation of labeled caspases using specific antisera. Cytosolic extracts (293) were activated by addition of cytochrome c/dATP for 10 min (+cyt c/dATP) and then labeled for 30 min with the general caspase probe KMB01 (20 μM) or directly labeled with KMB01 without activation (−cyt c/dATP). Caspases were precipitated by using specific antisera and analyzed by SDS-PAGE followed by blotting for biotin with streptavidin-HRP. I is input-labeled extracts, and P is the immunoprecipitated pellet. An asterisk (*) indicate crossreactive bands. Two asterisks (**) indicate forms of caspase-7 that are likely a result of the alternative transcription start site at methionine-45.

(C) Samples from (A) analyzed by immunoblot (IB) using caspase-7 and -9-specific antibodies. The identities of caspases are indicated based on immunoprecipitation experiments in (C). FL-C7 is full-length caspase-7, ΔN-C7 is full-length caspase-7 with the 23 N-terminal amino acids removed, p20 is mature large subunit of caspase-7 with N-terminal peptide removed, and p20+N-C7 is the mature large subunit of caspase-7 with N peptide intact. p35-C9 is the predominant autoprocessed mature form of caspase-9 large subunit, and p33-C9 is an alternatively processed form of the mature large subunit of caspase-9.

(D) Recombinant procaspase-7 (1 μM), expressed as described (Yang et al., 1998), was preincubated for 5 min with KMB01 (20 μM) and then incubated at 37°C without or with granzyme B (1:100 w/w ratio) for 30 min in hypotonic buffer containing 2 mM DTT. The labeling reaction was stopped by addition of SDS-PAGE sample buffer. A 20 μl portion was analyzed by immunoblot with a polyclonal caspase-7 antibody (anti-caspase-7 IB) and with streptavidin-HRP to detect the active site probe (ABP labeling). Because recombinant procaspase-7 efficiently processes its N peptide, the protein preparation is a mixture of full-length (37 kDa) and N peptide-processed (33 kDa) protein. The N peptide has no influence on the activation by GrB, activity, or labeling by ABPs.

(E) Immunoprecipitation of FL-C7 from etoposide-treated Jurkat cells. Cells (5×10^6) were treated with 1 μL of 2.5 μg/mL etoposide for 5 min before cell lysis and addition of 20 μM KMB01. FL-C7 was immunoprecipitated as in Figure 5B. I is input, P is pellet, and S is supernatant.

that they can gain direct access to the cytosol of cells and have potential for use as imaging agents. Surprisingly, KMB01 and bAB19 did not show labeling of the initiator caspases after etoposide or anti-Fas treatment. These findings may be in part due to the issue of cell permeability of the probe (for bAB19) or the potentially low levels and rapid turnover of active caspase-8 and -9 under these conditions. We are currently further exploring the applications of these new probes to intact cell systems.

Application of ABPs to Kinetic Studies of Caspase Activation in Apoptotic Proteomes

A cell-free extract system is ideal for temporal monitoring of both initiator and executioner caspase activity upon stimulation of the intrinsic apoptosis pathway. Caspase cleavage in this system has been studied extensively by using antibody-based detection methods and exogenous radiolabeled caspases (Liu et al., 1996; Orth et al., 1996; Rodriguez and Lazebnik, 1999; Slee et al., 1999; Srinivasula et al., 1998). We began by monitoring caspase activation in 293 cell extracts over a period of several hours after addition of cytochrome c/dATP (Figure 5A). Within the first 5–10 min of cytochrome c/dATP addition, robust labeling of the highly active downstream executioner caspases-3 and -7 (in the 17–22 kDa range) was observed. This activity peaked at 20–30 min and remained high throughout the duration of the experiment. In addition, a number of higher molecular weight bands around 35 kDa in size appeared early in the activation pathway. Immunoprecipitation of these labeled proteins identified the p37 and p32 species as forms of caspase-7 and the p35 and p33 as forms of caspase-9 (Figure 4B). This was further confirmed by the location of various intermediates of caspase-7 and -9 observed in the Western blots of the same samples (Figure 4C). The caspase-9 species labeled by KMB01 were assigned as the dominant p35 form of caspase-9 that results from autoprocessing of the zymogen at Asp315 (p35-C9) and a p33 form of caspase-9 that results from processing of the zymogen at an alternate residue in the linker region between the large and small subunits (p33-C9). In support of this assignment, a 33 kDa (p33) form of caspase-9 has also been observed in the recombinant enzyme as a result of cleavage within the E305/D306/E307 sequence in the linker region (Stennicke et al., 1999). Furthermore, addition of recombinant Bir3 domain of X-linked inhibitor of apoptosis protein (XIAP) (Srinivasula et al., 2001) blocked labeling of both the p35 and p33, but not the p37 or p32, forms of caspase-7 (Figure S2). We could also assign the identity of the p37 band as the full-length caspase-7 with intact N terminus (FL-C7) and the p32 species as the full-length caspase-7 with loss of the N-terminal peptide (ΔN-C7) (Denault and Salvesen, 2003).

The labeling of a full-length caspase-7 was unexpected, as this executioner caspase is thought to be activated in vivo only after removal of the N peptide by caspase-3 and processing of the zymogen to the large and small subunits by activity of the initiator caspases (Denault and Salvesen, 2003; Yang et al., 1998). However, we find that the full-length form of caspase-7 is capable of binding the active site probe and that the labeling of this species is enhanced by greater than 10-fold upon activation of the intrinsic death pathway (Figure 5C). We also reproducibly observed a small amount of probe-labeled FL-C7 in unactivated extracts, possibly resulting from the presence of low levels of active caspase-9 induced during preparation of the extracts. However, we cannot rule out the possibility that low levels of active FL-C7 exist constitutively within cells. Overall, these findings suggest that caspase-7 activation involves a catalytically active intermediate that was previously overlooked due to the inability to measure activity of the full-length zymogen in cytosolic extracts.

One possible hypothesis to explain the labeling of the full-length caspase-7 is that partial cleavage of the homodimeric zymogen upon stimulation of apoptosis results in a half-cleaved intermediate in which the uncleaved half becomes catalytically active as a result of structural rearrangements of the adjacent cleaved subunit. To test this hypothesis, we used recombinant granzyme B to activate recombinant zymogen caspase-7 (Yang et al., 1998) while monitoring labeling of the full-length caspase-7 using KMB01 (Figure 4D). In support of the half-cleaved intermediate, labeling of the full length caspase-7 was observed only after addition of granzyme B. Furthermore, this labeling of FL-C7 was lost when probe was added after granzyme B, suggesting that it is likely an intermediate in the activation pathway (data not shown). This observation also suggests that labeling of this intermediate requires activation through a proteolytic processing event and is not the result of a normally "floppy" linker region in the zymogen that allows incorporation of the probe.

Finally, to confirm the potential physiological relevance of this full-length intermediate, we set out to determine if it existed in intact cells that had been induced to undergo apoptosis by using different stimuli. Treatment of Jurkat cells with etoposide followed by labeling of cell lysates with KMB01 resulted in several probe-modified species, including one that was 37 kDa in size. This predominant p37 species was confirmed to be full-length caspase-7 by its immunoprecipitation using a specific antibody (Figure 4E). For a more detailed kinetic analysis of FL-C7 activation, Jurkat cells were treated with either etoposide or anti-Fas for a series of time intervals and labeling of endogenous caspases monitored by labeling of lysates from each time point with the probe KMB01 (Figure 4F). Interestingly, one of the primary probe-labeled species in the extracts at the early time points after activation by either etoposide or anti-Fas was the 37 kDa FL-C7. Similar to the extract system, this intermediate disappeared at later time points and accumulated when cells were pretreated

(F) Labeling of FL-C7 in CH11 (anti-Fas) and etoposide-treated Jurkat cells. Cells (5×10^6) were treated with CH11 or etoposide as in (D) and allowed to incubate for the time periods indicated. Cells were lysed in the presence of 20 μM KMB01, and lysates were labeled for 30 min at 37°C. The samples were then subjected to SDS-PAGE and blotted for biotin by using streptavidin-HRP and caspase-7 using specific antisera (see Experimental Procedures).

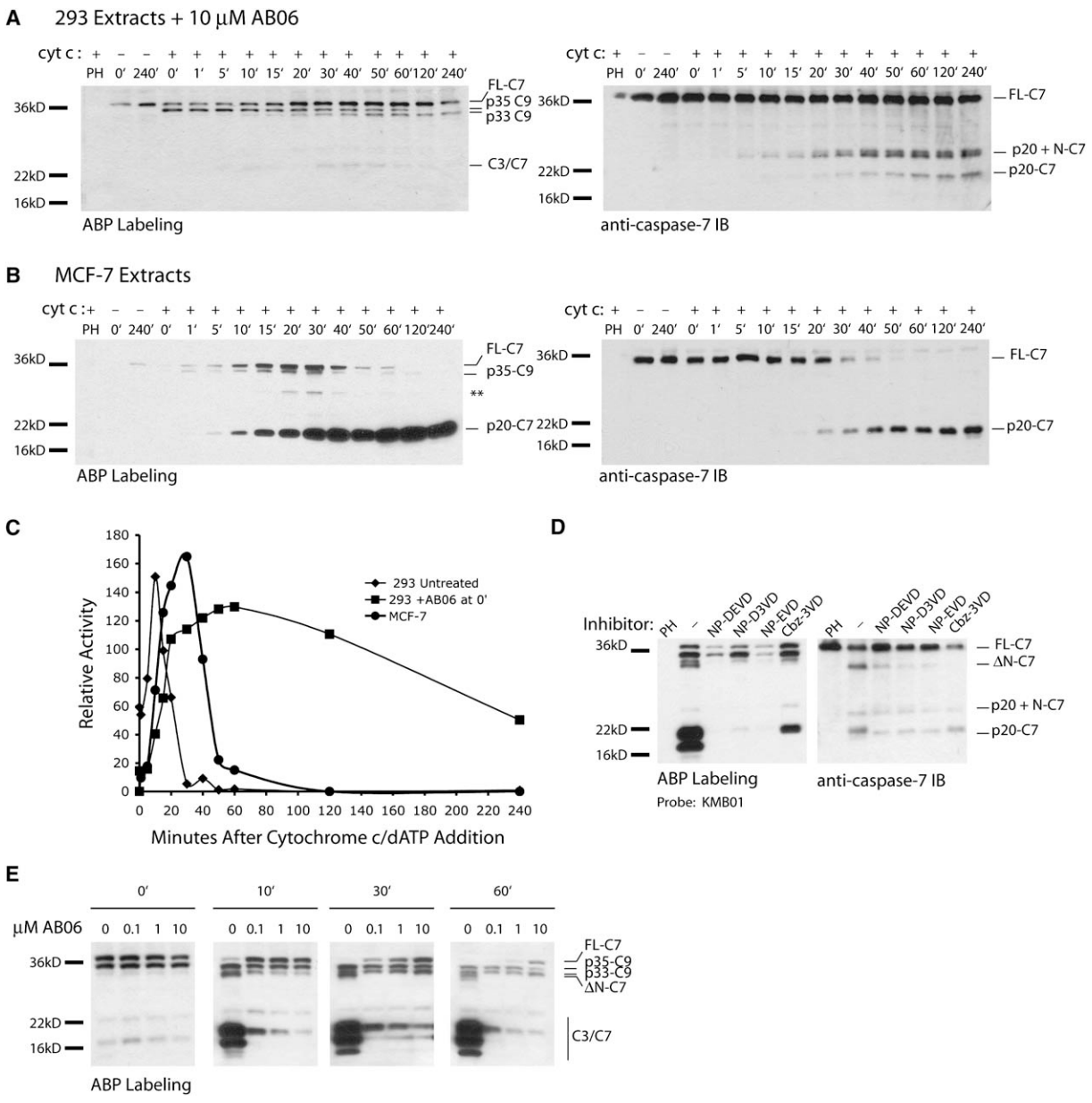

Figure 5. Full-Length Active Caspase-7 Has Unique Inhibitor Specificity and Is Processed to Mature Forms by Downstream Executioner Caspases

(A) The caspase-3-specific inhibitor AB06 causes accumulation of a catalytically active full-length form of caspase-7. Cytosolic extracts from 293 cells were activated with cytochrome c/dATP for the indicated times followed by labeling with KMB01 (left) and Western blotting with a caspase-7-specific antibody (right) as in Figure 4A.

(B) Full-length caspase-7 does not accumulate in cells lacking active caspase-3. The same experiment as (A) except extracts from MCF-7 cells were used in place of 293 extracts. Two asterisks (**) indicate forms of caspase-7 that are likely a result of the alternative transcription start site at methionine-45.

(C) Quantification of the relative activity of FL-C7 in uninhibited 293 extracts (from Figure 4S), AB06-treated 293 extracts (from [A]), and uninhibited MCF-7 extracts (from [B]).

(D) Inhibitor specificity of full-length and processed forms of caspase-7. Extracts (293) were activated for 5 min with cytochrome c/dATP and then incubated with inhibitors containing the indicated primary amino acid sequences for 5 min before KMB01 was added and allowed to label residual caspase active sites for 30 min. Samples were analyzed by SDS-PAGE followed by biotin blotting using strepavidin-HRP (left) or Western blotting for caspase-7 (right). Identities of labeled caspases are indicated.

(E) Specificity of AB06 after prolonged incubation times. Extracts were treated with AB06 at the indicated concentrations simultaneously with cytochrome c/dATP. At the indicated times after activation, samples were labeled with KMB01 (20 μM) for 30 min. Labeled caspases were resolved by SDS-PAGE analysis followed by biotin blotting using strepavidin-HRP.

with the caspase-3/7 selective inhibitor AB06 (Figure 4F). These data confirm that the results generated in extracts accurately mimic activation pathways observed in whole cells and suggest that the FL-C7 is a common intermediate in apoptosis pathways, which originate from different stimuli.

Application of Selective Inhibitors to Kinetic Studies of Caspase Activation in Apoptotic Proteomes

To examine a possible role for executioner caspases in the processing of upstream intermediates, we performed profiling experiments with the general probe KMB01 in 293 extracts in the presence or absence of the caspase-3 and -7-specific inhibitor AB06 (Figure 5A). We also performed the same experiment in MCF-7 cells, which lack active caspase-3 (Janicke et al., 2001), in order to separate processing events mediated by caspase-7 from those mediated by caspase-3 (Figure 5B).

Profiling of caspase activity in 293 extracts that had been treated with AB06 confirmed the selectivity of our inhibitor. Labeling of all mature downstream caspases (in the 17–22 kDa size range) was completely blocked, whereas labeling of the processed forms of caspase-9 and precursor forms of caspase-7 was unaltered. Interestingly, there was a dramatic change in the kinetics of activation of the full-length caspase-7 intermediate. In particular, active FL-C7 accumulated over time with a peak at 20 min that lasted until the end of the assay (Figures 5A and 5C). Activation of FL-C7 in MCF-7 cell extracts was slightly delayed but showed similar rates of accumulation and disappearance of active FL-C7 as those observed in uninhibited 293 extracts (Figures 5B and 5C). Together, these data suggest that activation of FL-C7 occurs through a process that is dependent on formation of the apoptosome but independent of the activation of mature forms of caspase-3 and -7. This hypothesis is supported by the fact that rates of formation of FL-C7 are relatively similar regardless of the status of mature executioner caspases (Figure 5C).

An additional surprising finding from the inhibitor studies was the overall lack of inhibition of the FL-C7 species by AB06 relative to mature p20 forms of caspase-7. This was surprising because the sequence of AB06 (NP-D3VD-AOMK) differs from the KMB01 probe sequence (Bio-Ahx-EVD-AOMK) only at the P3 residue. We reasoned that these data suggested that FL-C7 has a distinct active site topology that excludes binding of the more bulky P3 NN3 (2-pyridylalanine) residue. We therefore compared the ability of the inhibitors NP-DEVD-AOMK (AB09), NP-D3VD-AOMK (AB06), NP-EVD-AOMK, and Cbz-3VD-AOMK to bind to full-length and p20 mature forms of caspase-7 (Figure 5D). All four inhibitors efficiently blocked labeling of the mature p20 forms of caspase-7. In contrast, FL-C7 was relatively insensitive to inhibition by both inhibitors that contain NN3 in the P3 position and almost totally inhibited by the two inhibitors that contain a P3 Glu residue. We believe these data support the hypothesis that the FL-C7 contains an active site that allows restricted access to substrates. However, we cannot rule out the possibility that the observed change in selectivity to inhibitors is the result of overall reduced catalytic efficiency of the full-length intermediate relative to the mature processed form.

To confirm that our inhibitor AB06 was not reducing caspase-9 activity, resulting in slow processing of caspase-7 and accumulation of a partially processed intermediate, we treated extracts with a range of AB06 concentrations and monitored caspase-9 inhibition at various time points after cytochrome c/dATP addition (Figure 5E). These results confirmed the lack of cross-reactivity of AB06 even at concentrations as high as 10 μM for up to 30 min. Thus, the FL-C7 species is most likely an intermediate in the activation pathway that is normally rapidly processed by downstream caspases-3 and -7.

Discussion

Although significant progress has been made toward understanding biochemical properties such as substrate specificity and active site topology of caspases, there remains a lack of effective small molecules to monitor specific caspase targets in the context of a complex proteome, intact cell, or whole organism. Although several recent studies have made use of broad-spectrum activity based probes to monitor endogenous caspase activity in intact cells (Denault and Salvesen, 2003; Tu et al., 2006), the overall high reactivity of these reagents has prevented their use for real-time analysis of caspase activation. In this study, we developed highly selective active site probes and inhibitors that can be used to dissect these specific activation events. Using a positional scanning approach with peptide AOMKs containing both natural and nonnatural amino acids, we identified specificity elements that enabled the design of highly selective covalent inhibitors and active site probes. These compounds are likely to be valuable for in vitro studies of caspase activation and have the potential to be applied to in vivo imaging studies as reported for other classes of ABPs (Blum et al., 2005; Joyce et al., 2004).

We chose to apply our newly developed reagents to monitor caspases in cell-free extracts upon activation of the intrinsic death pathway. Although this system has been used extensively in the past, virtually all studies have relied on specific antibodies or exogenously added radiolabeled caspases to monitor the activation pathway. Thus, it is likely that critical activation events that occur independently of proteolytic processing have been overlooked. We therefore chose to use a general probe to label all forms of active caspases at various time points after stimulation of the extracts with cytochrome c/dATP. These initial kinetic studies produced several interesting findings. First, we found that the predominant active form of caspase-9 observed during activation of intrinsic apoptosis is likely the autocatalytic p35 form that results from cleavage at the Asp315 residue in the linker region. We also detected an active p33 form that results from alternate processing within the linker region. We did not detect the p37 form of caspase-9 that has been proposed to form through a caspase-3-mediated feedback loop (Slee et al., 1999). Furthermore, all forms of caspase-9 detected with the probes remained sensitive to inhibition by recombinant Bir3 domain, suggesting that none of these forms represent a constitutively active feedback product.

The second major finding was the appearance of a p37 full-length caspase-7 that becomes catalytically activated in extracts and intact cells upon stimulation of apoptosis pathways. The identification of a catalytically competent form of full-length caspase-7 without changes in total protein levels suggests that activation results from a specific structural change in the

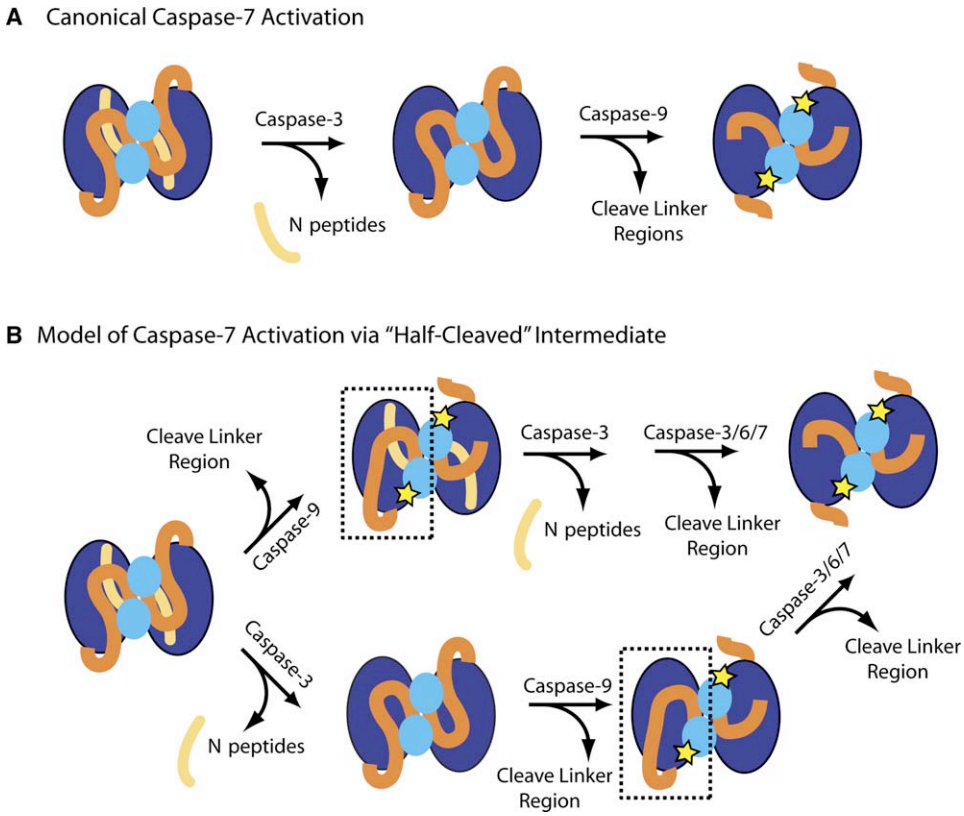

Figure 6. Revised Model of Caspase-7 Activation via a "Half-Cleaved" Intermediate

(A) Canonical model of caspase-7 activation in which N peptide (yellow region) is removed by caspase-3 followed by cleavage of the linker region (orange region) on both sides of the dimer by caspase-9 to produce the fully mature cleaved homodimer. In this model, cleavage of both linker regions of the dimer is required to generate the catalytic active site (star).

(B) Alternative model of caspase-7 activation in which initial processing of the uncleaved homodimer results in reorientation of the linker region and formation of a catalytically competent full-length caspase-7. This half-cleaved heterodimer is then a substrate for rapid processing by downstream executioner caspases-3, -6, or -7. Alternatively, the N peptide can be removed by caspase-3 followed by cleavage of the linker region to produce the half-cleaved complex. In both pathways, a catalytically active full-length caspase-7 is produced (dashed box).

uncleaved zymogen. The notion that the full-length caspase-7 could become catalytically active was surprising because executioner caspases are thought to initially form inactive homodimers that require cleavage between the large and small subunits by initiator caspases to become active (Boatright and Salvesen, 2003). In fact, high-resolution crystal structures of both zymogen and fully active mature forms of caspase-7 suggest that removal of the N peptide and cleavage within the flexible linker region between the large and small subunits is required to orient key catalytic residues in the active site (Chai et al., 2001; Riedl et al., 2001). However, the crystal structures obtained for caspase-7 as the fully uncleaved, inactive homodimer and fully cleaved, active homodimer represent "snap shots" or local starting and end points in the activation process. Intermediates that include a half-cleaved heterodimer are likely to exist but have yet to be characterized. Because the linker region where cleavage occurs is flexible, confirmation of the cleaved linker could exert allosteric control over the uncleaved zymogen, resulting in its activation. Evidence for such a half-cleaved caspase-7 heterodimer is supported by the work of Denault et al. reported in this issue (Denault et al., 2006). In these studies, various forms of caspase-7 that contain mutations that block either proteolytic processing of the linker region or the catalytic active site were used to generate half-cleaved heterodimers. These studies confirm an increase in probe labeling of an uncleaved full-length protein upon cleavage of the adjacent subunit. Furthermore, these studies are in agreement with our results obtained for labeling of the half-cleaved complex after granzyme B activation of the recombinant caspase-7 zymogen (Figure 4D). Thus, we believe that the increased labeling of the FL-C7 likely results from the partial processing of an inactive homodimer by initiators leading to at least partial formation of the active site in the uncleaved half (Figure 6). Because this activated form of full-length caspase-7 also shows distinct inhibitor binding properties, it may have a specific functional role in the apoptosis pathway or it may represent a relatively transient intermediate that does not act upon substrates. Importantly, this full-length form of caspase-7 appears to accumulate as the result of treatment of intact cells with different apoptotic stimuli, suggesting it may be the predominant intermediate in multiple forms of caspase-7-driven cell death pathways.

An additional significant finding was the accumulation of active FL-C7 upon inhibition of the mature forms of

caspase-3 and -7 using the newly developed selective inhibitor AB06. This is particularly interesting because active FL-C7 accumulates even at concentrations of inhibitor where the catalytic activity of caspase-9 is unaltered (Figure 5E). Our data suggest that although initial activation of FL-C7, most likely in the form of a half-cleaved complex, is mediated by initiator caspases, it cannot be efficiently processed by these enzymes to produce the fully cleaved mature homodimer. Furthermore, FL-C7 is processed with nearly normal kinetics in caspase-3-deficient MCF-7 cell extracts, suggesting that processing of FL-C7 to its mature forms is not caspase-3 dependent. Taken together, these results suggest that caspase-7 activation is a sequential process that involves the initial half-cleavage of a homodimer complex that is then released and further processed primarily by downstream caspase-7 activity.

The development of highly selective inhibitors and active site probes provides a means to selectively monitor the role of individual caspases during the process of apoptosis. Furthermore, the ability to monitor the temporal aspects of activation allows transient intermediates to be uncovered and their importance to be assessed. Our attention has now shifted to using these small molecule reagents to map out apoptosis pathways in more complex physiologically relevant systems.

Experimental Procedures

General Synthesis Methods

All inhibitors and ABPs were synthesized by solid phase synthesis methods previously reported for P1 Asp-AOMK compounds (Lee et al., 1999). All positional scanning peptide libraries were synthesized as reported previously (Greenbaum et al., 2002; Nazif and Bogyo, 2001) by reported synthesis methods for peptide AOMKs (Kato et al., 2005). All libraries were synthesized on a 50 μmol scale and assayed as crude mixtures after cleavage from the resin. Individual inhibitors and active site probes were synthesized on a 100 μmol scale and purified by using a C_{18} reverse-phase HPLC column (Delta-Pak, Waters Corp). Compound identity and purity were assessed by LC-MS analysis using an Agilent HPLC coupled to an API 150 mass spectrometer (Applied Biosystems/SCIEX) equipped with an ESI interface.

Library Screening

Library screening was carried out using recombinant caspases-3, -8, and -9 in caspase reaction buffer (100 mM Tris, 10 mM DTT, 0.1% CHAPS, and 10% sucrose [pH 7.4]). Caspases were preactivated by incubation in caspase reaction buffer for 15 min at 37°C before screening. Caspase-3 (10 nM), caspase-8 (20 nM), and caspase-9 (100 nM) were incubated at 37°C with inhibitor libraries. Concentrations of inhibitor libraries were selected such that they provided a spectrum of residual activity values ranging from 10% to 80% before normalization. For caspase-3, all libraries were screened at 50 nM final concentrations. For caspase-8, natural and nonnatural P2 and P4 libraries were screened at 50 nM whereas natural and nonnatural P3 libraries were screened at 500 nM final concentration. For caspase-9, all libraries were screened at 500 nM final concentration. After a 30 min incubation with the inhibitor libraries, 100 μM fluorescent substrate (DEVD-AFC for caspase-3, LETD-AFC for caspase-8, and LEHD-AFC for caspase-9, Calbiochem) was added and reactions incubated for 15 min. Endpoint fluorescent readings (Abs 495 nm/Emis 515 nm) were measured by using a Spectramax M5 plate reader (Molecular Devices). Relative fluorescence values were converted to percentages of residual activity relative to uninhibited controls. Values were internally normalized such that lowest percent residual activity was adjusted to 0% and highest percent residual activity was adjusted to 100%. Residual activity values were compared by using hierarchical clustering as described (Greenbaum et al., 2000, 2002; Nazif and Bogyo, 2001).

Kinetic Compound Screening

Compound screening was completed by using the progress curve method as described (Salvesen, 1989). All screening was carried out in caspase reaction buffer. The caspase-9-specific compounds AB38, 40, 41, and 42 were screened in caspase reaction buffer and in caspase buffer with 1 M sodium citrate instead of sucrose as described (Pop et al., 2006). The concentrations of active caspases used were as follows: 5 nM active caspase-3, 5 nM active caspase-7, 10 nM active caspase-8, and 50 nM active caspase-9. To ensure full activation, caspases-3/7, -8, and -9 were preincubated at 37°C for 5, 10, or 40 min, respectively, before kinetic measurements were made.

Biotin and Caspase-7 and -9 Immunoblots

All protein samples were quenched in SDS sample buffer and boiled for 5 min at 90°C before SDS-PAGE analysis. Samples were separated on 10%–20% Tris-Glycine gradient gels (Novex, Invitrogen) as indicated. Proteins were transferred to nitrocellulose (BioRad) membranes. All biotin and caspase-9 blots were blocked for 1 hr in PBST-5% Milk solution , and all caspase-7 blots were blocked in PBST-3% BSA. Biotin blots were subsequently washed for 30 min in PBST followed by a 45 min incubation in 1:3500 dilution of Streptavidin-HRP (Sigma) in PBST. Caspase-9 blots were incubated overnight in a 1:3000 dilution of the polyclonal caspase-9 antibody AR-19B (Burnham Institute for Medical Research) (Stennicke et al., 1999) or a 1:2000 dilution of polyclonal caspase-7 (Cell Signaling Technologies, cat # 9492) in PBST-5% Milk solution or PBST-3% BSA. After 2 × 30 min washes in PBST, antibody blots were incubated in 1:3000 dilution of secondary anti-rabbit (Santa Cruz) in PBST-5% Milk or PBST-3% BSA for 30 min. All blots were washed 3 × 5min in PBST and visualized by using Supersignal West Pico Chemiluminescent Substrate (Pierce).

Competition and Direct Labeling of Recombinant Caspases

For all competition and direct labeling experiments recombinant caspases were pre-incubated in caspase reaction buffer for 15 min at 37°C. For competition experiments, 100 nM of active site titrated caspase was incubated for 30 min at 37°C with appropriate inhibitor and then residual active sites were labeled with 5 μM KMB01 for an additional 30 min. For direct labeling, 100 nM of caspase-3, -8, and -9 was incubated together in the presence of appropriate ABPs at the indicated concentrations for 30 min at 37°C.

Cell Culture

Jurkat and MCF-7 cells were cultured in RPMI 1640 supplemented with 10% fetal calf serum (FCS), 2 mM glutamine, 100 U/ml penicillin, and 100 μg/ml streptomycin and maintained in 5% CO_2 at 37°C. 293 cells were cultured as above except DMEM was used in place of RPMI 1640.

Hypotonic Extract Preparation

Hypotonic 293 and MCF-7 extracts were prepared as described previously (Liu et al., 1996).

Direct Labeling of Endogenous and Exogenous Caspases in Apoptotic 293 and MCF-7 Extracts

Protein concentration of hypotonic extracts was measured by using a standard Bradford Protein Assay (BioRad). 293 extracts were obtained at a total protein concentration of 4.7 μg/μL, and MCF-7 extracts were diluted to this concentration. Cytochrome c (100 μM final) and dATP (1 mM final) were added to extracts (73 μg of total protein in a final volume of 20 μL) at time zero, and incubation was continued at 37°C for 10 min ABPs (at final concentrations indicated) were added, and labeling continued for an additional 30 min. Samples (13.5 μg of total protein) were analyzed on 10%–20% Tris-Glycine gradient gels (Novex Invitrogen). Alternatively, recombinant caspase-8 (100 nM) was added to 293 extracts (as above) in conjunction with cytochrome c/dATP (as above) where appropriate. Extracts were labeled with 10 μM of KMB01, bAB19, and bAB38 10 min after activation/caspase-8 addition for 30 min at 37°C. Samples (as above) were analyzed as above by SDS-PAGE using 10%–20% gradient gels (as above).

Direct Labeling of Endogenous Caspase Activity in Live Jurkat cells

Cells (3×10^6) in media (1 ml) were treated with etoposide (2.5 μg; Calbiochem) or anti-Fas antibody (0.5 μg; clone CH11, Upstate Signaling Solutions) for 15 hr. Cells were then incubated for 2 hr with 10 μM final concentrations of KMB01, bVAD-fmk, (Calbiochem), or bAB19 or 1 μM final concentrations of bAB06 or bAB13 for 2 hr. Cells were washed three times in cold PBS and lysed by boiling in 4× SDS sample buffer for 5 min at 90°C. Labeled proteins were analyzed by SDS-PAGE, and blotting was as described above.

Intrinsic Apoptosis Assay in Cell Extracts

Hypotonic 293 or MCF-7 extracts (4.7 μg/μl total protein concentration; 73 μg of total protein per time point) were activated by addition of cytochrome c (100 μM final) and dATP (1 mM final) for a range of times from 0 to 240 min as indicated. KMB01 (20 μM final) or vehicle control (DMSO) was added at the end of the indicated activation time, and labeling was carried out for an additional 30 min at 37°C. Samples were quenched by addition of 4× SDS sample buffer followed by boiling for 5 min. A portion (13.5 μg total protein) from each time point was analyzed by SDS-PAGE using 10%–20% gradient gels followed by blotting for biotin as described above.

Intrinsic Apoptosis Assay in Cell Extracts in the Presence of Exogenous Bir3

Hypotonic 293 extracts (73 μg of total protein) were activated as described above and allowed to incubate for the indicated times. Recombinant, purified Bir 3 (1 μM) was added to extracts where appropriate, and incubation continued for an additional 5 min before addition of KMB01 (20 μM final). Labeling was carried out for an additional 30 min, and samples (13.5 μg total protein) were analyzed by SDS-PAGE and biotin blotting as described above.

Quantification of Labeling of FL-C7 in Hypotonic 293 Extracts

The intensity of KMB01 labeling of FL-C7 in timecourse assays was quantified by using the publicly available program ImageJ (http://rsb.info.nih.gov/ij/).

Inhibitor Specificity of FL-C7 in Hypotonic 293 Extracts

Hypotonic 293 extracts (73 μg of total protein) were activated at 37°C for 5 min as described above. NP-EVD-AOMK, NP-DEVD-AOMK (AB09), NP-D3VD-AOMK, or NP-3VD-AOMK (20 μM final) was added to extracts for 5 min before KMB01 (20 μM final) was added and allowed to incubate for 30 min at 37°C. Samples (13.5 μg total protein) were analyzed by SDS-PAGE and biotin blotting as described above.

Titration of AB06 in Hypotonic 293 Extracts

Hypotonic 293 extracts were activated as described above, and AB06 was added after 5 min to the final concentrations indicated. After a 5 min incubation, KMB01 (20 μM final) was added and allowed to incubate for 30 min. All reactions were carried out at 37°C.

Immunoprecipitation

Protein A/G agarose beads (40 μL) were preincubated with 5 μg of the indicated antibody overnight in 300 μl IP buffer (1× PBS [pH 7.4], 0.5% NP-40, and 1 mM EDTA) at 4°C. Antibodies used were as follows: H-277 caspase-3 poly-clonal (cat #: sc-7148, Santa Cruz) and caspase-7 monoclonal (cat# 556541, BD-Pharmingen), caspase-9 AR-19B (Stennicke et al., 1999). After being washed three times in IP buffer, beads were resuspended in 300 μL IP buffer and sample was added and allowed to incubate with shaking overnight at 4°C. Beads were washed three times in IP buffer followed by three times in 0.9% NaCl. Beads were boiled in 1× sample buffer for 15 min. All supernatant samples were acetone precipitated for 2 hr at −80°C, dried, and resuspended in 1× sample buffer. All samples were subjected to SDS-PAGE followed by biotin blot as described above.

Supplemental Data

Supplemental Data include two figures and two tables and can be found with this article online at http://www.molecule.org/cgi/content/full/23/4/509/DC1/.

Acknowledgments

We thank A. Price, S. Snipas, F. Scott, C. Pop, and B. Eckelman for technical assistance and production of recombinant caspases. This work was supported by a Turman Fellowship at Stanford University (to M.B.), a National Institutes of Health (NIH) National Technology Center for Networks and Pathways grant U54 RR020843 (to M.B.), NIH grant R01-EB005011 (to M.B.), NIH grant R01-NS37878 (to G.S.S.), and a Department of Defense Breast Cancer Center of Excellence grant DAMD-17-02-0693 (to Bonnie Sloane—M.B. subcontract). A.B.B. was funded by a National Human Genome Research Institute training grant, 5T32 HG00044.

Received: March 31, 2006
Revised: June 5, 2006
Accepted: June 13, 2006
Published: August 17, 2006

References

Backes, B.J., Harris, J.L., Leonetti, F., Craik, C.S., and Ellman, J.A. (2000). Synthesis of positional-scanning libraries of fluorogenic peptide substrates to define the extended substrate specificity of plasmin and thrombin. Nat. Biotechnol. *18*, 187–193.

Blum, G., Mullins, S.R., Keren, K., Fonovic, M., Jedeszko, C., Rice, M.J., Sloane, B.F., and Bogyo, M. (2005). Dynamic imaging of protease activity with fluorescently quenched activity-based probes. Nat. Chem. Biol. *1*, 203–209.

Boatright, K.M., and Salvesen, G.S. (2003). Mechanisms of caspase activation. Curr. Opin. Cell Biol. *15*, 725–731.

Boatright, K.M., Renatus, M., Scott, F.L., Sperandio, S., Shin, H., Pedersen, I.M., Ricci, J.E., Edris, W.A., Sutherlin, D.P., Green, D.R., and Salvesen, G.S. (2003). A unified model for apical caspase activation. Mol. Cell *11*, 529–541.

Chai, J., Wu, Q., Shiozaki, E., Srinivasula, S.M., Alnemri, E.S., and Shi, Y. (2001). Crystal structure of a procaspase-7 zymogen: mechanisms of activation and substrate binding. Cell *107*, 399–407.

Denault, J.B., and Salvesen, G.S. (2002). Caspases: keys in the ignition of cell death. Chem. Rev. *102*, 4489–4500.

Denault, J.B., and Salvesen, G.S. (2003). Human caspase-7 activity and regulation by its N-terminal peptide. J. Biol. Chem. *278*, 34042–34050.

Denault, J.-B., Békés, M., Scott, F.L., Sexton, K.M.B., Bogyo, M., and Salvesen, G.S. (2006). Engineered hybrid dimers: tracking the activation pathway of caspase-7. Mol. Cell *23*, this issue, 523–533.

Deveraux, Q.L., Stennicke, H.R., Salvesen, G.S., and Reed, J.C. (1999). Endogenous inhibitors of caspases. J. Clin. Immunol. *19*, 388–398.

Garcia-Calvo, M., Peterson, E.P., Leiting, B., Ruel, R., Nicholson, D.W., and Thornberry, N.A. (1998). Inhibition of human caspases by peptide-based and macromolecular inhibitors. J. Biol. Chem. *273*, 32608–32613.

Greenbaum, D., Medzihradszky, K.F., Burlingame, A., and Bogyo, M. (2000). Epoxide electrophiles as activity-dependent cysteine protease profiling and discovery tools. Chem. Biol. *7*, 569–581.

Greenbaum, D.C., Arnold, W.D., Lu, F., Hayrapetian, L., Baruch, A., Krumrine, J., Toba, S., Chehade, K., Bromme, D., Kuntz, I.D., and Bogyo, M. (2002). Small molecule affinity fingerprinting. A tool for enzyme family subclassification, target identification, and inhibitor design. Chem. Biol. *9*, 1085–1094.

James, K.E., Asgian, J.L., Li, Z.Z., Ekici, O.D., Rubin, J.R., Mikolajczyk, J., Salvesen, G.S., and Powers, J.C. (2004). Design, synthesis, and evaluation of aza-peptide epoxides as selective and potent inhibitors of caspases-1, -3, -6, and -8. J. Med. Chem. *47*, 1553–1574.

Janicke, R.U., Engels, I.H., Dunkern, T., Kaina, B., Schulze-Osthoff, K., and Porter, A.G. (2001). Ionizing radiation but not anticancer drugs causes cell cycle arrest and failure to activate the mitochondrial death pathway in MCF-7 breast carcinoma cells. Oncogene *20*, 5043–5053.

Joyce, J.A., Baruch, A., Chehade, K., Meyer-Morse, N., Giraudo, E., Tsai, F.Y., Greenbaum, D.C., Hager, J.H., Bogyo, M., and Hanahan, D. (2004). Cathepsin cysteine proteases are effectors of invasive growth and angiogenesis during multistage tumorigenesis. Cancer Cell *5*, 443–453.

Kato, D., Boatright, K.M., Berger, A.B., Nazif, T., Blum, G., Ryan, C., Chehade, K.A., Salvesen, G.S., and Bogyo, M. (2005). Activity-based probes that target diverse cysteine protease families. Nat. Chem. Biol. *1*, 33–38.

Lee, A., Huang, L., and Ellman, J.A. (1999). General solid-phase method for the preparation of mechanism-based cysteine protease inhibitors. J. Am. Chem. Soc. *121*, 9907–9914.

Liu, X., Kim, C.N., Yang, J., Jemmerson, R., and Wang, X. (1996). Induction of apoptotic program in cell-free extracts: requirement for dATP and cytochrome c. Cell *86*, 147–157.

Nazif, T., and Bogyo, M. (2001). Global analysis of proteasomal substrate specificity using positional-scanning libraries of covalent inhibitors. Proc. Natl. Acad. Sci. USA *98*, 2967–2972.

Orth, K., O'Rourke, K., Salvesen, G.S., and Dixit, V.M. (1996). Molecular ordering of apoptotic mammalian CED-3/ICE-like proteases. J. Biol. Chem. *271*, 20977–20980.

Pop, C., Timmer, J., Sperandio, S., and Salvesen, G. (2006). The apoptosome activates caspase-9 by dimerization. Mol. Cell *22*, 269–275.

Reed, J.C. (1998). Dysregulation of apoptosis in cancer. Cancer J. Sci. Am. *4* (Suppl 1), S8–S14.

Riedl, S.J., Fuentes-Prior, P., Renatus, M., Kairies, N., Krapp, S., Huber, R., Salvesen, G.S., and Bode, W. (2001). Structural basis for the activation of human procaspase-7. Proc. Natl. Acad. Sci. USA *98*, 14790–14795.

Rodriguez, J., and Lazebnik, Y. (1999). Caspase-9 and APAF-1 form an active holoenzyme. Genes Dev. *13*, 3179–3184.

Salvesen, G.S., and Nagase, H. (1989). Proteolytic Enzymes. a Practical Approach (Oxford: IRL Press).

Slee, E.A., Harte, M.T., Kluck, R.M., Wolf, B.B., Casiano, C.A., Newmeyer, D.D., Wang, H.G., Reed, J.C., Nicholson, D.W., Alnemri, E.S., et al. (1999). Ordering the cytochrome c–initiated caspase cascade: hierarchical activation of caspases-2, -3, -6, -7, -8, and -10 in a caspase-9-dependent manner. J. Cell Biol. *144*, 281–292.

Srinivasula, S.M., Ahmad, M., Fernandes-Alnemri, T., and Alnemri, E.S. (1998). Autoactivation of procaspase-9 by Apaf-1-mediated oligomerization. Mol. Cell *1*, 949–957.

Srinivasula, S.M., Hegde, R., Saleh, A., Datta, P., Shiozaki, E., Chai, J., Lee, R.A., Robbins, P.D., Fernandes-Alnemri, T., Shi, Y., and Alnemri, E.S. (2001). A conserved XIAP-interaction motif in caspase-9 and Smac/DIABLO regulates caspase activity and apoptosis. Nature *410*, 112–116.

Stennicke, H.R., Deveraux, Q.L., Humke, E.W., Reed, J.C., Dixit, V.M., and Salvesen, G.S. (1999). Caspase-9 can be activated without proteolytic processing. J. Biol. Chem. *274*, 8359–8362.

Stennicke, H.R., Renatus, M., Meldal, M., and Salvesen, G.S. (2000). Internally quenched fluorescent peptide substrates disclose the subsite preferences of human caspases 1, 3, 6, 7 and 8. Biochem. J. *350*, 563–568.

Thornberry, N.A., Peterson, E.P., Zhao, J.J., Howard, A.D., Griffin, P.R., and Chapman, K.T. (1994). Inactivation of interleukin-1 beta converting enzyme by peptide (acyloxy)methyl ketones. Biochemistry *33*, 3934–3940.

Thornberry, N.A., Rano, T.A., Peterson, E.P., Rasper, D.M., Timkey, T., Garcia-Calvo, M., Houtzager, V.M., Nordstrom, P.A., Roy, S., Vaillancourt, J.P., et al. (1997). A combinatorial approach defines specificities of members of the caspase family and granzyme B. Functional relationships established for key mediators of apoptosis. J. Biol. Chem. *272*, 17907–17911.

Tu, S., McStay, G.P., Boucher, L.M., Mak, T., Beere, H.M., and Green, D.R. (2006). In situ trapping of activated initiator caspases reveals a role for caspase-2 in heat shock-induced apoptosis. Nat. Cell Biol. *8*, 72–77.

Yang, X., Stennicke, H.R., Wang, B., Green, D.R., Janicke, R.U., Srinivasan, A., Seth, P., Salvesen, G.S., and Froelich, C.J. (1998). Granzyme B mimics apical caspases. Description of a unified pathway for trans-activation of executioner caspase-3 and -7. J. Biol. Chem. *273*, 34278–34283.